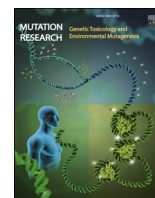


Contents lists available at [ScienceDirect](https://www.sciencedirect.com)

# Mutation Research - Genetic Toxicology and Environmental Mutagenesis

journal homepage: [www.elsevier.com/locate/gen tox](http://www.elsevier.com/locate/gen tox)

## Blood molecular profile to predict genotoxicity from exposure to antineoplastic drugs

Carina Ladeira<sup>a,b,c,\*</sup>, Rúben Araújo<sup>c,d,f</sup>, Luís Ramalhte<sup>d,e,f</sup>, Hélder Teixeira<sup>d</sup>,  
Cecília R.C. Calado<sup>d,g</sup>

<sup>a</sup> H&TRC – Health & Technology Research Center, Escola Superior de Tecnologia da Saúde de Lisboa (ESTeSL), Instituto Politécnico de Lisboa, Avenida D. João II, lote 4.69.01, Parque das Nações, 1990-096 Lisboa, Portugal

<sup>b</sup> NOVA National School of Public Health, Public Health Research Centre, Universidade NOVA de Lisboa, Lisbon, Portugal

<sup>c</sup> Comprehensive Health Research Center (CHRC), Universidade NOVA de Lisboa, Portugal

<sup>d</sup> ISEL – Instituto Superior de Engenharia de Lisboa, Instituto Politécnico de Lisboa, R. Conselheiro Emídio Navarro 1, 1959-007 Lisboa, Portugal

<sup>e</sup> Blood and Transplantation Center of Lisbon, Instituto Português do Sangue e da Transplantação, Alameda das Linhas de Torres, no 117, 1769-001 Lisbon, Portugal

<sup>f</sup> NOVA Medical School, Faculdade de Ciências Médicas, Universidade NOVA de Lisboa, 1169-056 Lisbon, Portugal

<sup>g</sup> CIMOSM - Centro de Investigação em Modelação e Otimização de Sistemas Multifuncionais, ISEL - Instituto Superior de Engenharia de Lisboa, Instituto Politécnico de Lisboa, R. Conselheiro Emídio Navarro 1, 1959-007 Lisboa, Portugal

### ARTICLE INFO

#### Keywords:

Molecular profile  
FTIR-spectroscopy  
Genotoxicity  
Cytokinesis-blocked micronucleus assay  
Frozen blood  
Antineoplastics

### ABSTRACT

Genotoxicity is an important information that should be included in human biomonitoring programmes. However, the usually applied cytogenetic assays are laborious and time-consuming, reason why it is critical to develop rapid and economic new methods. The aim of this study was to evaluate if the molecular profile of frozen whole blood, acquired by Fourier Transform Infrared (FTIR) spectroscopy, allows to assess genotoxicity in occupational exposure to antineoplastic drugs, as obtained by the cytokinesis-block micronucleus assay. For that purpose, 92 samples of peripheral blood were studied: 46 samples from hospital professionals occupationally exposed to antineoplastic drugs and 46 samples from workers in academia without exposure (controls). It was first evaluated the metabolome from frozen whole blood by methanol precipitation of macromolecules as haemoglobin, followed by centrifugation. The metabolome molecular profile resulted in 3 ratios of spectral bands, significantly different between the exposed and non-exposed group ( $p < 0.01$ ) and a spectral principal component-linear discriminant analysis (PCA-LDA) model enabling to predict genotoxicity from exposure with 73 % accuracy. After optimization of the dilution degree and solution used, it was possible to obtain a higher number of significant ratios of spectral bands, *i.e.*, 10 ratios significantly different ( $p < 0.001$ ), highlighting the high sensitivity and specificity of the method. Indeed, the PCA-LDA model, based on the molecular profile of whole blood, enabled to predict genotoxicity from the exposure with an accuracy, sensitivity, and specificity of 92 %, 93 % and 91 %, respectively. All these parameters were achieved based on 1  $\mu\text{L}$  of frozen whole blood, in a high-throughput mode, *i.e.*, based on the simultaneous analysis of 92 samples, in a simple and economic mode. In summary, it can be concluded that this method presents a very promising potential for high-dimension screening of exposure to genotoxic substances.

### 1. Introduction

Genotoxicity refers to the ability of harmful substances - chemical, physical, and biological - to interact with genetic material, which can result in genomic instabilities and multiple mutations which are associated with various diseases, namely cancer [1]. Therefore, this

information is often the key contributor to the understanding of carcinogenicity and other genetic diseases, being widely used in safety risk assessment of chemicals, together with general toxicity, carcinogenicity, reproductive toxicity, and other endpoints [2]. Monitoring genotoxicity in occupational and environmental surveillance programmes is extremely important, since it allows the detection of early effects that

\* Corresponding author at: H&TRC – Health & Technology Research Center, Escola Superior de Tecnologia da Saúde de Lisboa (ESTeSL), Instituto Politécnico de Lisboa, Avenida D. João II, lote 4.69.01, Parque das Nações, 1990-096 Lisboa, Portugal.

E-mail address: [carina.ladeira@estesl.ipl.pt](mailto:carina.ladeira@estesl.ipl.pt) (C. Ladeira).

<https://doi.org/10.1016/j.mrgentox.2023.503681>

Available online 18 August 2023

1383-5718/© 2023 The Authors. Published by Elsevier B.V. This is an open access article under the CC BY license (<http://creativecommons.org/licenses/by/4.0/>).

result from the interaction between the individual and the environment, enabling tackle health risks derived from exposure, usually complex chemical mixtures [3–5].

Cytogenetic methods are important in the search for DNA damage, resulting from environmental and occupational exposure to chemical pollutants and physical factors, such as ionizing radiation [6]. The cytokinesis-block micronucleus (CBMN) assay is a comprehensive system for measuring DNA damage, cytostasis and cytotoxicity. DNA damage events are scored specifically in once-divided binucleated (BN) cells and include (i) micronuclei (MNI), a biomarker of chromosome breakage and/or whole chromosome loss, (ii) nucleoplasmic bridges (NPBs), a biomarker of DNA misrepair and/or telomere end-fusions, and (iii) nuclear buds (NBUDs), a biomarker of elimination of amplified DNA and/or DNA repair complexes [7]. It is a quite dynamic assay, since it has been continuously evolving as a molecular cytogenetic method of chromosomal instability [8]. The CBMN assay is often used on blood samples *in vitro/ex-vivo* to study genotoxic effects of chemicals (reviewed in [9]), demonstrating its continuous importance for the future as one of the most reliable, well established and feasible genotoxicity tests [10]. The information about *in vitro* genotoxicity testing by MN is gathered, revised and systematized in the Organization for Economic Co-operation and Development (OECD) 487 Guideline [11]. Despite CBMN assay being less laborious, expensive and time consuming, in comparison with chromosomal aberrations technique, the procedure can take up to 5 days to complete [7].

The ideal method for routine genotoxicity monitoring should be rapid, simple, economic, applicable in high-throughput measurements, and with high sensitivity and specificity predictive values. Fourier-Transform Infrared (FTIR) spectroscopy, associated to multivariate data analysis, presents diverse characteristics that may enable to achieve that requirements. The technique reflects vibrations between atoms in molecules - related to atoms and atoms environment, thus providing information concerning the biochemical composition of the analysed system [12]. The molecular fingerprint acquired by the technique, associated to data analysis, has been explored to predict very specific and sensitive analysis, including cell differentiation [13], mechanisms of cell death [14], bacteria typing at genus, species and strain level [15], diseases diagnosis and prognosis, oxidative stress [16–18], cytotoxic [19,20] and genotoxic effects evaluation [20–22]. The analysis pointed before has been conducted in cells, tissue and biofluids [22–24].

Advantages of FTIR spectroscopy include its versatility in detection modes, e.g., the analysis in high-throughput based on microplates with multi-wells (from 96 to 1056), measuring microvolumes from 25 to 1  $\mu$ L, where the spectra of one sample can be acquired in 1 min, with minimal sample processing (e.g.: dehydration step with inexpensive reagents). In a previous work, it was predicted from a drop of serum by FTIR spectra, the genotoxicity information from the occupational exposure to antineoplastic drugs - Cyclophosphamide (CP), 5-Fluorouracil (5-FU) and Paclitaxel (PTX) - in hospital professionals, and compared with CBMN assay results obtained [22]. A support vector machine model of serum spectra enabled to predict genotoxicity with high accuracy (91 %), however, to achieve these results whole blood should be maintained and transported in cold storage ( $\approx 4$  °C), between 24 and 48 h, until laboratorial analysis. If blood centrifugation and analysis is not possible to be conducted during the first 48 h after blood collection, blood should be frozen, e.g., at  $-20$ °C, for the days to weeks until analysis. Advantages of analysing frozen whole blood, pertain to the increased coverage of the population that can be analysed. Since the method used only requires a drop of blood, the discomfort and risks associated to blood collection can be also minimised. To simplify the method previously developed [22] and enable its application, even when centrifugation is not possible to obtain serum, the present work evaluated the use of FTIR spectroscopy in frozen whole blood to predict genotoxicity.

Freezing blood will lead to cell lysis, and the higher content of erythrocytes ( $\approx 5$  million per mL), and leukocytes ( $\approx 5000$  cells per mL), can impair the models predictivity. The FTIR-spectroscopic analysis of

whole blood will include not only DNA damage from leukocytes, but also metabolites and other macromolecules from the extracellular compartment of blood, leukocytes, erythrocytes, and platelets. Therefore, genotoxic prediction will not be based on direct relationship between genotoxicity (i.e., DNA damage), but mostly from indirect relationship between genotoxicity and general metabolism. For example, the relationship between diverse drugs on genotoxicity, oxidative stress and lipid peroxidation is well known [25–29], and even on the metabolic impact of blood composition [23] and erythrocytes [30]. In general, antineoplastic drugs can induce oxidative stress. CP may impair redox balance in tissues, suggesting that biochemical and physiological disorders can be caused by oxidative stress [31] and a particular study that identified erythrocytotoxicity, which is characterized by oxidative stress and dyslipidaemia [32]. Also 5-FU induced an increase in ROS levels both *in vivo* and *in vitro* [33,34]. Finally, PAX mechanism of action also goes by inducing oxidative stress and suppressing cell viability and number [35,36].

In the present work, it was evaluated the prediction of genotoxicity from the direct analysis of frozen whole blood. For that purpose, it was assessed the univariate spectral analysis, the ratios of spectral bands of the two groups of volunteers – 46 hospital professionals occupationally exposed to the previously mentioned drugs, significantly presenting an increase of genotoxic biomarkers in relation to 46 non-exposed subjects [37,38]. It was also conducted a multivariate data analysis, as spectra principal components analysis (PCA), to search for data patterns, and supervised processing method based on PCA-Linear Discriminant Analysis (PCA-LDA), based on PCA scores to assign the samples to their predicted groups, i.e., exposed *versus* non-exposed.

Since most of the frozen whole blood contains lysed erythrocytes, and consequently a high quantity of haemoglobin ( $\approx 95$  % erythrocyte dry cell weight is haemoglobin) and platelets, it was also evaluated the impact of blood, particles and macromolecules removal. With that purpose, it was used methanol to induce macromolecules precipitation followed by centrifugation, as usually conducted to obtain the metabolome from serum and plasma [39]. After that, models to predict the exposure to genotoxic compounds from methanol-based extraction and frozen whole blood, based on spectra PCA-LDA, were compared.

## 2. Materials and methods

### 2.1. Subjects of study

The human volunteers participating in the current study were described in previous publications of Ladeira et al. [37,38]. The study was conducted in accordance with standards of ethics and received the necessary approvals (ACT project 036APJ/09) from the institution's administrations and from each study participant with the informed consent form. Peripheral blood was collected by venipuncture from 46 hospital workers occupationally exposed to antineoplastic drugs – pharmacists, pharmacy technicians and nurses – and from 46 volunteers from academia without this exposure (controls). Both groups were apparently healthy and not statistically different in relation to sex and alcohol drinking habits. The controls were slightly older ( $p = 0.006$ ), with an average age of  $39 \pm 10$  years old in comparison to exposed group with  $34 \pm 8$  years old; and presented a higher number of smokers ( $p = 0.08$ ), with 9 regular smokers in relation to 4 regular smokers from the exposed group.

### 2.2. CBMN assay

CBMN assay was conducted as described in Ladeira et al. [37]. Briefly, mononuclear cells were isolated from whole peripheral blood by gradient isolation (Ficoll-Paque, Sigma-Aldrich), and subsequently processed according to Fenech [7]. The cells were observed by optical microscopy after air drying cells, in microscope slides and double-stained with May–Grünwald–Giemsa and mounted with

Entellan®. Two slides were analysed per sample, each one was coded and analysed by an observer accordingly with the criteria described by Fenech et al. [40]. Statistical analysis of diverse variables between the groups were conducted by a Mann-Whitney U test (with IBM's SPSS).

### 2.3. FTIR-spectroscopic analysis

Whole blood with EDTA anticoagulant was maintained several weeks at - 80 °C until analysis. On the day of FTIR spectroscopic analysis, frozen whole blood samples were defrosted, vortexed and diluted at 1/10, 1/20 and 1/40 (v/v) in NaCl 0.9 % (w/v) (Sigma). In some experiments, blood was diluted in phosphate buffer saline at pH 7.4, (PBS, contained 137 mM NaCl, 2.7 mM KCl, 8 mM Na<sub>2</sub>HPO<sub>4</sub>, and 2 mM KH<sub>2</sub>PO<sub>4</sub>), or was previously centrifuged (10 min, 14,000 rpm, 4°C) (Mikro, with rotor 1195/L, Hettich Zentrifugen) before spectra acquisition.

Metabolites extraction was conducted by mixing 150 µL of frozen whole blood with 225 µL of methanol (Fisher Chemical), which was subsequently vortexed for 30 s, and after 10 min resting was centrifuged for 10 more minutes, at 14,000 rpm, 4°C (Mikro, with rotor 1195/L, Hettich Zentrifugen). The supernatant was diluted at ½ (v/v) with NaCl 0.9 % (w/v).

FTIR spectroscopic analysis was based on transmission detection mode, associated to a high-throughput reading system and all samples

were analysed in triplicate. Briefly, triplicates of 25 µL of each sample were transferred to a 96-wells Si plate and dehydrated for about 2.5 h in a desiccator under vacuum (Vacuubrand, ME 2). Spectral data was collected using a FTIR-spectrometer (Vertex 70, Bruker) equipped with an HTS-XT (Bruker) accessory. Each spectrum represented 64 coadded scans, with a 2 cm<sup>-1</sup> resolution, and was collected in transmission mode, between 400 and 4000 cm<sup>-1</sup>. The first well of the plate did not contain a sample and the corresponding spectra was acquired and used as background, according to the HTS-XT manufacturer.

Spectra were pre-processed by offset baseline correction, unit-vector normalization and second derivative using a Savitzky-Golay filter, with a 2nd order polynomial over a 15-point window. Spectra PCA, based on NIPALS algorithm, and PCA-LDA were conducted. Spectra pre-processing and processing were conducted with The Unscrambler® X, version 10.4 (CAMO software AS, Norway). Signal noise was determined by the highest absorbance spectral band divided by the standard deviation of noise between 1900 and 2000 cm<sup>-1</sup>. Student's *t*-Test was applied to ratios of baseline corrected spectral bands, using Microsoft Excel™.

### 3. Results and discussion

The hospitals from which the exposed professionals worked, presented surfaces contaminated with one of the three studied drugs, or

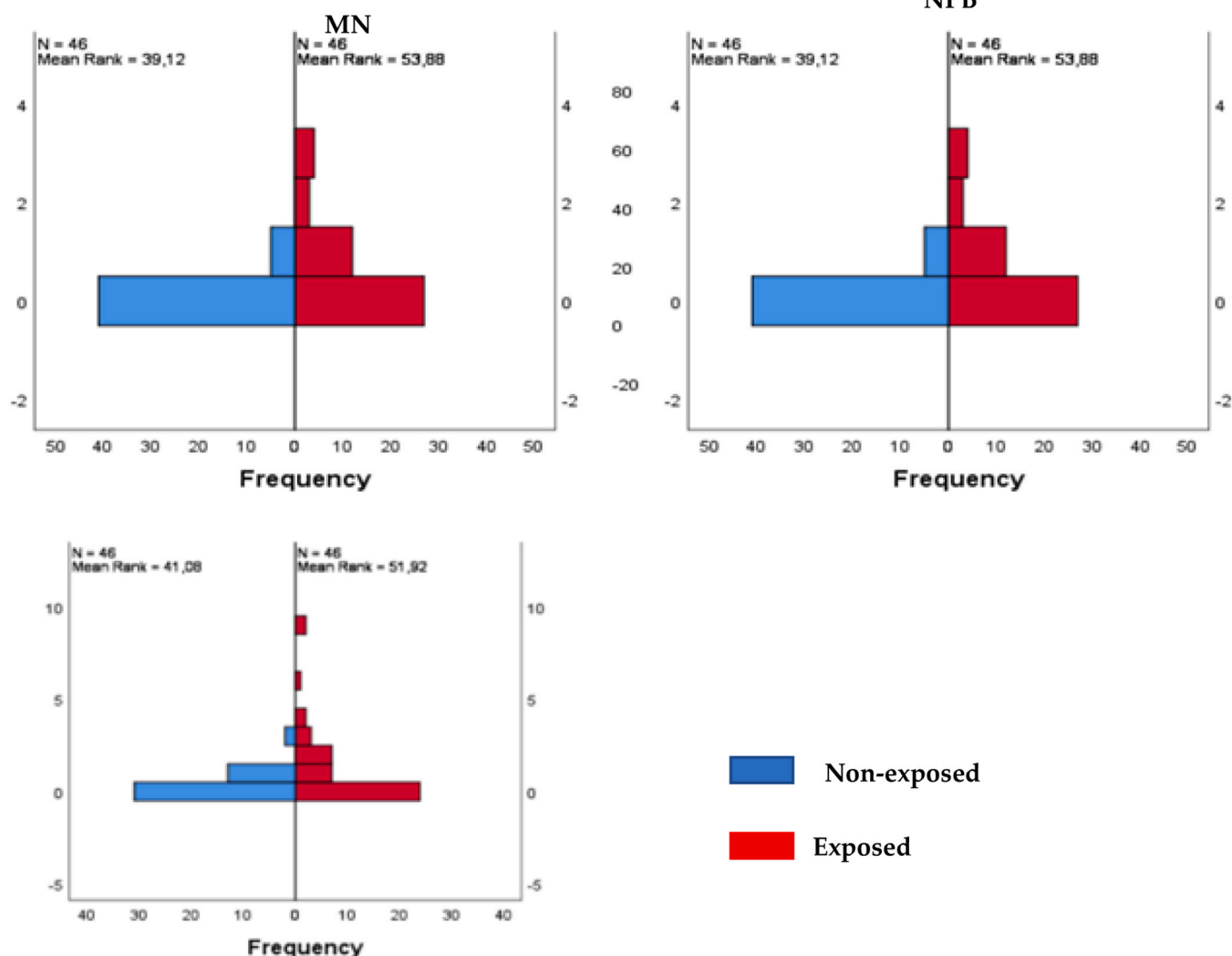


Fig. 1. Frequency of MN, NPB and NBUD in non-exposed (blue bars) and exposed (red bars) subjects.

with more than one drug. The detailed data of antineoplastic agents' exposure assessment was previously published in Viegas et al. [41] and Ladeira et al. [37]. Oncology nurses and other healthcare staff in oncology units are at risk of exposure to antineoplastic agents. Although many contamination routes can be considered [42], it would seem that contact with contaminated surfaces and also permeation of gloves can be the predominant route of exposure due to dermal absorption [42–46]. With respect to genotoxicity, it was found significant increases of all the genotoxicity biomarkers measured in exposed subjects in comparison with non-exposed (Fig. 1), with *p*-values based on Mann-Whitney U test < 0.0001, 0.01 and 0.06 for MN, NPB and NBUD, respectively. A significant increase of MN frequency in professionals handling antineoplastic drugs was also observed in other studies [47–52].

### 3.1. Methanol based extracts from frozen whole blood

Frozen whole blood contains the result of lysed cells, mostly erythrocytes, haemoglobin and cells membranes. After blood defrosting, methanol was added to precipitate macromolecules [39], followed by centrifugation to eliminate particles and precipitated macromolecules. The supernatant spectra (Fig. 2A), and corresponding PCA were acquired (Fig. 2B).

The ratios of the main spectral bands from baseline corrected spectra were analysed, as the ratios between bands allow artefacts elimination due to sample quantity and baseline contribution underneath each band (Table 1). Bands at the following regions were evaluated [53–56]: 2800–3000  $\text{cm}^{-1}$ , from stretching vibrations of  $\text{CH}_2$  and  $\text{CH}_3$  groups mostly from lipids; 1720–1780  $\text{cm}^{-1}$ , due to  $\text{C}=\text{O}$  vibrations of fatty acids, triglycerides and cholesterol esters; 1320–1370  $\text{cm}^{-1}$ , due to  $\text{CH}_2$  and  $\text{CH}_3$  deformation of lipids and proteins; 1500–1670  $\text{cm}^{-1}$ , mostly due to amide I and II vibrations from peptides; 1070–1090  $\text{cm}^{-1}$ , from symmetric stretching of  $\text{PO}_2$  – from nucleic acids, phospholipids and saccharides; 1400–1480  $\text{cm}^{-1}$ , from diverse group vibrations as from  $\text{COO}^-$ ,  $\text{CH}_2$  and amide III from peptides, and some bands from the fingerprint region, associated to a high diversity of functional groups. Statistically significant differences of ratios in spectral bands ( $p < 0.01$ ) were observed between the two groups of volunteers, some with high statistical significance (Table 2): the 1121/1040 ratio ( $p = 0.001$ ), due to stretching vibrations of  $\text{C}-\text{O}$  and  $\text{C}-\text{O}-\text{C}$  of carbohydrates; the 1735 / 1621 ratio ( $p = 0.003$ ), due to stretching vibrations of  $\text{C}=\text{O}$  of fatty acids, triglycerides and cholesterol esters, in relation to amide III in peptides, respectively; and due to 861/773 ratio ( $p = 0.004$ ) from bands from the fingerprint region.

To further evaluate if methanol-based extracts enabled to predict individual's genotoxic effects from exposure to antineoplastic drugs, a spectra PCA was conducted, to search for data patterns (Fig. 2B). The PCA score plot based on baseline corrected spectra points to some degree of separation between the two groups of samples but, since no clear data

**Table 1**

Mean and standard deviation of spectral bands from methanol obtained extracts from frozen blood from hospital professionals occupationally exposed to anti-neoplastic drugs in comparison with controls (without exposure).

Spectral band	Group	Mean	Standard deviation	<i>p</i> -value
2961/2921	Exposed	0.947	0.069	0.014
	Non-exposed	0.967	0.083	
2921 / 2875	Exposed	1.285	0.121	0.034
	Non-exposed	1.316	0.169	
2875 / 2852	Exposed	0.944	0.060	>0.1
	Non-exposed	0.954	0.087	
1657 / 1557	Exposed	1.886	0.345	>0.1
	Non-exposed	1.919	0.491	
1557 / 1519	Exposed	1.873	0.334	>0.1
	Non-exposed	1.898	0.469	
1519 / 1504	Exposed	1.342	0.146	0.044
	Non-exposed	1.376	0.181	
1735 / 1621	Exposed	0.187	0.099	0.003
	Non-exposed	0.150	0.075	
1460 / 1448	Exposed	0.926	0.059	0.069
	Non-exposed	0.908	0.059	
1412 / 1354	Exposed	1.307	0.249	0.025
	Non-exposed	1.368	0.257	
1353 / 1324	Exposed	1.374	0.234	> 0.1
	Non-exposed	1.348	0.251	
1258 / 1089	Exposed	0.682	0.182	0.027
	Non-exposed	0.739	0.288	
1262 / 1124	Exposed	0.770	0.181	> 0.1
	Non-exposed	0.794	0.245	
1089 / 1121	Exposed	1.155	0.306	> 0.1
	Non-exposed	1.132	0.229	
1121 / 1040	Exposed	1.134	0.237	0.001
	Non-exposed	1.246	0.345	
861 / 773	Exposed	0.585	0.103	0.004
	Non-exposed	0.548	0.127	
931 / 861	Exposed	0.796	0.138	0.036
	Non-exposed	0.828	0.160	
993 / 931	Exposed	0.941	0.185	> 0.1
	Non-exposed	0.923	0.188	
1041 / 993	Exposed	1.525	0.471	> 0.1
	Non-exposed	1.603	0.564	

separation was observed on PCA, a supervised processing method was applied, based on PCA-LDA analysis (Table 2). The performance of the PCA-LDA models to predict genotoxicity from exposure was determined by the model's accuracy, sensitivity, and specificity. Sensitivity points to the rate of predicting the true exposed individuals among all predicted exposed individuals, whereas specificity points to the rate of predicting the true non-exposed individuals in relation to all predicted non-exposed individuals. The accuracy points to the rate of predicting true exposed and true non-exposed individuals.

To achieve the best PCA-LDA model, the impact of the following spectra pre-processing methods on the model performance were

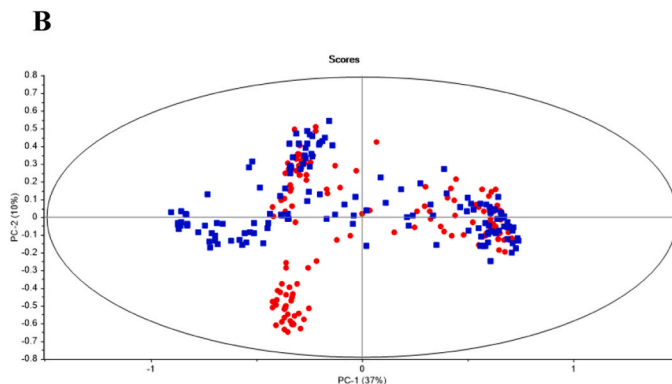
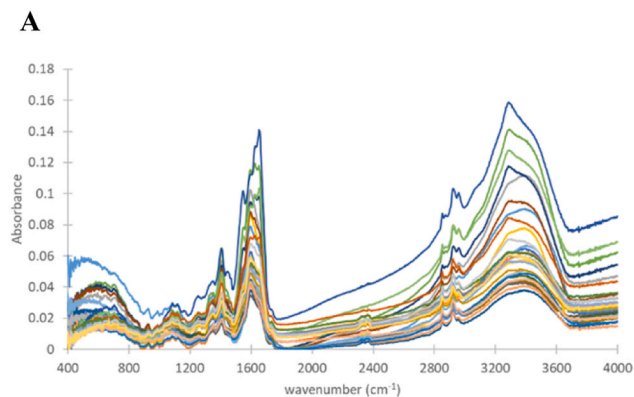


**Fig. 2.** Example of spectra without pre-processing of methanol-based extracts from defrosted whole blood (A) and PCA based on normalised second derivative spectra of exposed (blue) in relation to non-exposed volunteers (red) (B).

**Table 2**

Performance of PCA-LDA models to predict individuals' genotoxic effects from exposure to antineoplastic drugs from methanol-based extracts, obtained from frozen blood, according to spectral regions and spectra pre-processing based on baseline correction (BC) normalization (UVN) and second derivative (2D).

Spectra pre-processing	Spectral region (cm <sup>-1</sup> )	Accuracy (%)	Sensitivity (%)	Specificity (%)
BC	400–4000 (whole spectra)	65	70	59
BC & UVN	whole spectra	64	65	64
2D & UVN	whole spectra	67	68	67
	600–1800 + 2800–3000	64	65	64
	2800–3000	64	53	75
	600–1800	60	70	50
	600–1300	73	66	80
	600–1500	65	58	71
	1500–1800	62	69	55

evaluated: baseline corrected (method I), baseline corrected followed by normalization (method II) and normalised second derivative (method III). Normalisation minimises the effect of sample quantity, and consequently the effect of experimental procedure variation, highlighting the sample biochemical composition. Normalised second derivative spectra was also evaluated since derivatives can resolve superimposed bands and increase the acquired information. However, since derivatives can also increase spectra noise, when derivatives were used, sub-regions of the spectra with less noise, such as the one between 600 and 1800 and 2800–3000 cm<sup>-1</sup> were also evaluated (Table 2), including between 2800 and 3000 cm<sup>-1</sup>, representing CH<sub>2</sub> and CH<sub>3</sub> group vibrations from lipids, the sub-region between 600 and 1800 cm<sup>-1</sup>, including the fingerprint region representing complex combinations of vibrations of diverse functional groups, and other bands as from phosphate groups (≈1080 and 1240 cm<sup>-1</sup>) from nucleic acids, phospholipids and phosphorylated proteins, amide group vibrations from peptides (≈1500–1700 cm<sup>-1</sup>), CH<sub>2</sub> and CH<sub>3</sub> vibrations from lipids as phospholipids and proteins (≈1380, 1395 and 1450 cm<sup>-1</sup>), carbohydrates (between 950 and 1070 cm<sup>-1</sup>), among others [56].

The best PCA-LDA models from methanol-based extracts (Table 2), were built on normalised second derivative spectra (method III) between 600 and 1300 cm<sup>-1</sup> region, presenting an accuracy, sensitivity, and specificity of 73 %, 66 % and 80 % respectively. This model performance was, however, much lower than the one previously obtained with serum (with an accuracy of 91 % [22]). Due to this, it was subsequently evaluated the direct analysis of frozen whole blood, *i.e.*, without methanol precipitation, that ultimately results in a much simpler process.

### 3.2. Frozen whole blood

To achieve spectra with a high signal-to-noise ratio (S/N), while minimising signal saturation, it was evaluated the effect of the dilution and solution used before spectra acquisition. During the dehydration step, required before spectra acquisition, it is important to achieve a homogenous dry film on each well of the microplate, to reduce diffraction phenomena [57,58], which can impair spectra quality and hinder the performance of the models to predict genotoxicity. The solution used to dilute the blood can affect the process, therefore it was evaluated NaCl and PBS solutions. The concentration used gave a much lower signal in comparison with diluted blood samples (data not shown). Since the presence of particles can also impair spectra quality, blood was centrifuged to remove possible particles from cell lysis. In order to assess all these aspects, a preliminary assay was conducted to evaluate the impact of the blood centrifugation, the degree of blood dilution, and the use of NaCl or PBS for the dilution (Fig. 3, Table 3).

Table 3 presents the mean of the signal-to-noise ratio of 5 quintuplicate spectra obtained with a sample diluted with NaCl or PBS at a range of dilutions from 1/8–1/40, with or without centrifugation before spectra acquisition. It is also shown the mean and standard deviation obtained for all 1800 wavenumbers of the 5 quintuplicate spectra. Table 3 also presents the sum of the mean values of all wavenumbers divided by 1800 for normalization purposes. It was observed that independent of dilution degree and solution, centrifugation resulted in an increased signal, probably due to particles reduction and, consequently, diffraction events. However, centrifugation also resulted in an increase of standard deviation, which led to a reduction of S/N in 5 out of the 7 conditions evaluated. Based on these preliminary results, the following work was based on non-centrifuged blood.

For non-centrifuged blood, dilution with NaCl in relation to PBS and for the same dilution degree, resulted in a lower signal (*i.e.*, M) and lower standard deviation and, consequently, on a much higher S/N

**Table 3**

Effect of blood dilution degree, dilution solution and centrifugation before spectral acquisition on the mean of noise signal ratio (S/N) of 5 quintuplicate spectral analysis. The mean and standard deviation (SD) refers to the sum of the mean and standard deviation of all wavenumbers, divided by 1800 for normalization.

Dilution	Solvent used	dilution	Non-centrifuged			Centrifuged		
			Mean	SD	S/N	Mean	SD	S/N
PBS solution		1/8	0.193	0.018	3200	0.203	0.035	2500
		1/10	0.131	0.030	700	0.161	0.012	1500
		1/15	0.125	0.014	1500	0.126	0.030	200
		1/20	0.081	0.007	250	0.081	0.008	200
NaCl solution		1/10	0.126	0.023	7000	0.137	0.028	2600
		1/20	0.040	0.004	600	0.089	0.022	400
		1/40	0.025	0.004	400	0.032	0.002	800

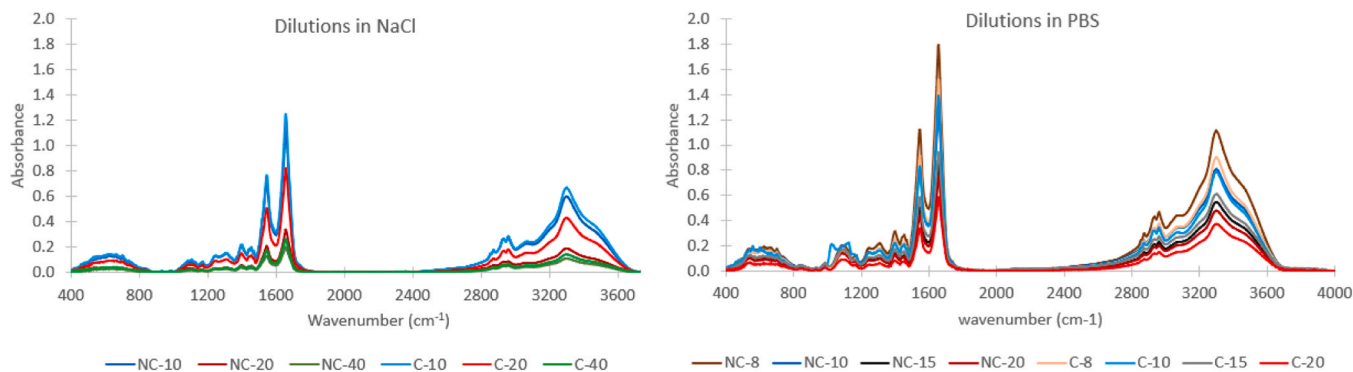


**Fig. 3.** Average FTIR spectra of quintuplicate analysis of blood samples that were centrifuged (C) or not centrifuged (NC) and diluted in NaCl or PBS solutions from 1/8–1/40.

(Table 3). Therefore, the remaining work was conducted with blood diluted in NaCl solution.

Since a higher dilution degree usually leads to a reduction of both standard deviation and S/N, in the following work, the effect of blood dilution in NaCl continued to be evaluated. From the spectral ratios evaluated, the dilution at 1/40 resulted in a higher number of significant bands ratios between the two groups of volunteers (Table 4). Interestingly, the worst results were obtained with the intermediate dilution, *i. e.*, at 1/20. Most probably, this result is due to the dilution at 1/10 leading to the highest S/N, where at 1/40 it most probably maximises information retrieval from the spectra due to minimisation of saturation of some bands.

The most significant bands ratios ( $p < 0.00001$ ) were observed (Table 4, Fig. 3) in the region between 2800 and 3000  $\text{cm}^{-1}$ , from stretching vibrations of  $\text{CH}_2$  and  $\text{CH}_3$  groups, mostly from lipids (*e.g.*, 2955/2868); 1238/1051 due to asymmetric stretching from  $\text{PO}_2$  from lipids, nucleic acids and phosphorylated proteins and from C-O-P from phosphate ester, respectively; 1122/1101, from C-O from carbohydrates; 1081/1051, from symmetric stretching from  $\text{PO}_2$  and C-O-P from phosphate ester, respectively. A much higher significant difference was observed in ratios of spectral bands of whole blood in relation to the methanol extracts.

To further explore the use of frozen blood to predict genotoxic effects from exposure to antineoplastic drugs, the spectra PCA was conducted (Fig. 4). PCA score plot points that the increased dilution degree (from 10 to 40) leads to a decrease in scores dispersion, according to the reduced standard deviation for higher dilution degrees pointed on Table 4. This was observed with non-derivative and derivative spectra (Fig. 4). However, since a higher score dispersion could be related to a higher sensitivity in acquiring molecular fingerprints, associated to the volunteer physiological state, the PCA-LDA models built to predict the

genotoxic effects from exposure to antineoplastic drugs were based on the three different dilution degrees (Table 4).

The impact of the following spectra pre-processing methods on the PCA-LDA predicting models was conducted, as previously, on baseline corrected, baseline corrected followed by normalisation or normalised second derivative. When comparing these three spectra pre-processing methods over the three dilution degrees (1/10, 1/20 and 1/40), the samples diluted at 1/20 presented the lowest accuracies, around 70 %, whereas, with a dilution of 1/10 or 1/40 it presented accuracies between 77 % and 82 %. The highest sensitivities were also achieved with dilution at 1/10 and 1/40 (Table 5). This was according to the lowest number of significant ratios of bands being observed at the 1/20 dilution.

Since the second derivative spectra also increased noise signal which can impair model performance, when using the derivative spectra, it was also evaluated spectral sub-regions. From all pre-processing methods and subregions evaluated, the PCA-LDA models with the higher accuracies ( $> 90\%$ ) were obtained with a dilution factor of 1/40 and based on normalised second derivative spectra between 600 and 1300  $\text{cm}^{-1}$  (of 92 %) or between 600 and 1500  $\text{cm}^{-1}$  (of 91 %). The other complementary sub-regions were evaluated at this dilution factor, as the one including the amide group vibrations from peptides (*e.g.*, between 1500 and 1800  $\text{cm}^{-1}$ ) among others. But neither of these sub-regions presented higher accuracies when compared to the region between 600 and 1300  $\text{cm}^{-1}$ . The model based on normalised second derivative on this region presented an accuracy, sensitivity, and specificity of 92 %, 93 % and 91 %, respectively; predicting genotoxic effects to exposure to antineoplastic drugs. These values were even slightly higher than the ones obtained from serum spectra based on a support vector machine, that resulted in accuracy, sensitivity and specificity of 91 %, 90 % and 86 %, respectively [22].

**Table 4**

Mean and standard deviation of spectral bands from frozen blood, previously diluted at 1/40 on NaCl solution of occupationally exposed workers to antineoplastic drugs in comparison with controls (without exposure). The *p*-value of a Student's *t*-test comparing, in mean terms, the spectral band ratios between the two groups of volunteers is present for samples diluted at 1/40, 1/20 and 1/10 is presented.

Spectral band	Group	Dilution at 1/40			Dilution at 1/10	Dilution at 1/20
		Mean	Standard deviation	<i>p</i> -value		
2955/2926	Exposed	1.005	0.026	0.39	0.06	0.3
	Non-exposed	0.996	0.033			
2868/2864	Exposed	1.058	0.011	<0.00001	0.13	0.0003
	Non-exposed	1.068	0.007			
2955/2868	Exposed	1.449	0.073	<0.00001	<0.00001	<0.00001
	Non-exposed	1.497	0.040			
2955/2864	Exposed	1.534	0.089	<0.00001	<0.00001	<0.00001
	Non-exposed	1.600	0.046			
1659/1541	Exposed	1.480	0.045	0.012	0.09	0.07
	Non-exposed	1.448	0.044			
1659/1238	Exposed	5.765	0.874	0.0004	0.008	0.09
	Non-exposed	5.336	0.726			
1541/1238	Exposed	3.900	0.548	0.0005	0.001	0.1
	Non-exposed	3.679	0.413			
1659/1395	Exposed	3.972	0.411	0.00007	0.009	0.01
	Non-exposed	3.711	0.411			
1659/1465	Exposed	4.891	0.582	0.006	0.01	0.09
	Non-exposed	4.593	0.496			
1541/1465	Exposed	3.299	0.339	0.009	0.002	0.1
	Non-exposed	3.165	0.258			
1541/1395	Exposed	2.682	0.223	0.00003	0.001	0.008
	Non-exposed	2.557	0.216			
1453/1380	Exposed	1.187	0.040	0.003	0.002	0.2
	Non-exposed	1.186	0.028			
1238/1051	Exposed	1.734	0.377	<0.00001	<0.00001	<0.00001
	Non-exposed	1.535	0.158			
1165/1101	Exposed	0.928	0.055	0.04	0.03	0.5
	Non-exposed	0.916	0.025			
1122/1101	Exposed	0.887	0.029	<0.00001	<0.00001	<0.00001
	Non-exposed	0.919	0.034			
1081/1051	Exposed	1.327	0.116	<0.00001	<0.00001	0.0002
	Non-exposed	1.280	0.062			

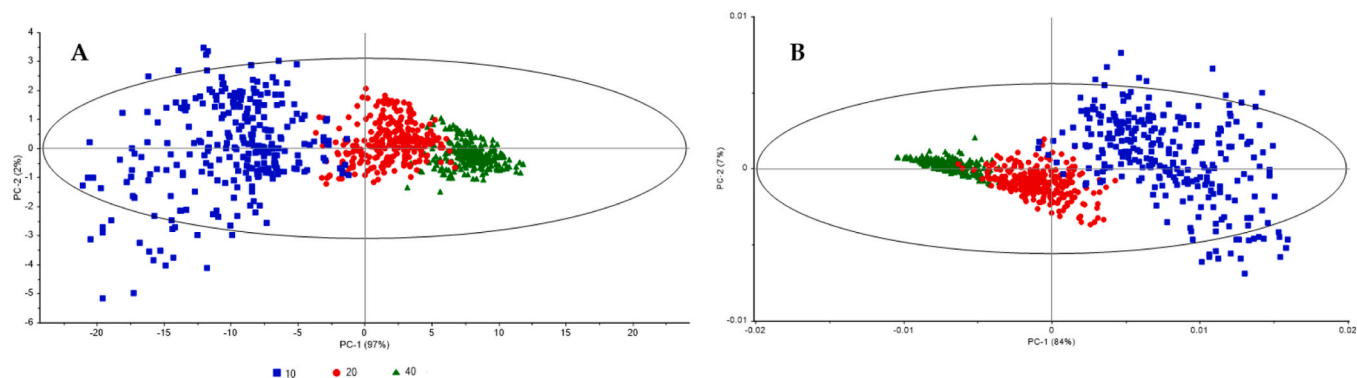


**Fig 4.** PCA of baseline corrected spectra (A), or the second derivative spectra (B) of non-centrifuged whole blood samples diluted with NaCl solution at 1/10 (blue), 1/20 (red) and 1/40 (green). The Hotelling's  $T^2$  ellipse is at 1 % significance.

**Table 5**

Performance of PCA-LDA models to predict genotoxicity from exposure to antineoplastic drugs from spectra of frozen whole blood according to the dilution in NaCl solution, spectral regions and spectra pre-processing based on baseline correction (BC) normalization (UVN) and second derivative (2D).

Dilution	Spectra pre-processing	Spectral region ( $\text{cm}^{-1}$ )	Accuracy (%)	Sensitivity (%)	Specificity (%)		
1/40	BC	400–4000 (whole spectra)	78	85	73		
		whole spectra	80	78	82		
	BC & UVN	2800–3000	78	74	84		
		600–1800	68	73	65		
		600–1300	69	72	65		
		600–1500	73	81	66		
		2D & UVN	whole spectra	66	62	71	
			600–1800 + 2800–3000	74	75	72	
			2800–3000	77	82	72	
			600–1800	82	80	85	
			<b>600–1500</b>	91	95	88	
			1500–1800	80	82	79	
		1/20	BC	whole spectra	69	73	65
				whole spectra	70	69	72
BC & UVN	whole spectra		70	73	67		
	600–1800 + 2800–3000		67	70	64		
	2800–3000		64	63	66		
	<b>600–1300</b>		76	72	80		
	600–1500		74	77	72		
	2D & UVN		whole spectra	82	91	71	
			whole spectra	77	85	70	
	1/10		BC	whole spectra	81	87	76
whole spectra		74		78	70		
BC & UVN		600–1800 + 2800–3000	77	81	74		
		2800–3000	77	81	74		
		<b>600–1300</b>	80	80	80		
		600–1500	77	83	70		

#### 4. Conclusions

Monitoring genotoxicity of occupational and environmental exposures, is critical, either for professional safety assurance or to epidemiological studies, *e.g.*, to discover new exposure sources. However, large-scale monitoring processes will be strongly promoted only if an alternative method, enabling to predict genotoxicity, based on rapid, economic, and simple procedures, but also highly sensitive and specific, is developed. The present work describes a new method based on the analysis of frozen whole blood by FTIR spectroscopy, followed by multivariate data analysis. To enable the application of the new method on economic and large-scale analysis, blood samples were analysed in a high-throughput mode, using a microplate system, enabling the analysis of 96 up to 1056 samples. Also, the analysis from non-centrifuged frozen whole blood presents advantages such as the simplicity and coverage increase of population under study, since blood can be obtained even without centrifugation. In this case, blood can be frozen and sent for

laboratory analysis. Furthermore, the analyses can be based in less than a drop of blood, since the best predicting models were based on the analysis of 20  $\mu\text{L}$  of blood previously diluted at 1/40, requiring therefore less than 1  $\mu\text{L}$  of blood. This low amount of blood can be obtained even by a prick blood sample test, reducing the discomfort usually associated to blood collection.

It was evaluated the impact of macromolecules elimination by blood pre-processing with methanol followed by centrifugation and blood dilution, solution used and need for blood centrifugation during analysis. Data was analysed by univariate analysis, based, for example, on analysis of ratios between spectral bands, and multivariate analysis, as based on non-supervised (*i.e.*, PCA) and supervised (*i.e.*, PCA-LDA) algorithms. In summary, the best predicting model of individual exposure to genotoxic compounds was observed in frozen whole blood, non-centrifuged nor pre-processed with methanol, simply diluted at 1/40 in NaCl solution, and considering the normalised second derivative spectra between the region 600–1300  $\text{cm}^{-1}$ , which resulted in an

accuracy, sensitivity, and specificity of 92 %, 93 % and 91 %, respectively. With these results and given the fact that the analyses were conducted with less than 1 µL of whole blood and 96-wells microplate was used; this study presents very promising outputs for a future and robust genotoxicity monitoring platform applicable at large-scale.

It is important to address that despite these encouraging results, it should be highlighted that this method is based on indirect prediction of genotoxicity based on whole blood molecular composition, on contrary to methods such as the CBMN assay which directly analyses DNA damage. Therefore, it is critical to validate the results in future studies based on large scale populations, using as references, direct assays such as CBMN. Also, these studies should include a higher diversity of groups to evaluate the possible impact on the blood molecular fingerprint such as habits, e.g., food, drinking, smoking, and other variables, such as sex, age and physiopathological states.

### Institutional Review Board Statement

The study was conducted in accordance with the Declaration of Helsinki and approved by the hospital administration board. Informed consent was obtained from all subjects involved.

### Funding

This work was supported by Instituto Politécnico de Lisboa under grant IDI&CA/IPL/2021/PLASCOGEN\_ESTeSL, IDI&CA/IPL/2017/GenTox/ESTeSL, and by the *Fundação para a Ciência e a Tecnologia*, Portugal, under grant DSAIPA/DS/0117/2020. The human biomonitoring had financial support given by Portuguese Authority of Working Conditions (Project reference: 036APJ/09).

### CRedit authorship contribution statement

All authors contributed equally on the conceptualization of the manuscript. All authors have read and agreed to the published version of the manuscript.

### Declaration of Competing Interest

The authors declare that they have no known competing financial interests or personal relationships that could have appeared to influence the work reported in this paper.

### Data Availability

Data will be made available on request.

### References

- N. Ren, M. Atyah, W.-Y. Chen, C.-H. Zhou, The various aspects of genetic and epigenetic toxicology: testing methods and clinical applications, *J. Transl. Med* 15 (2017) 110, <https://doi.org/10.1186/s12967-017-1218-4>.
- M. Hayashi, Opinion: regulatory genotoxicity: past, present and future, *Genes Environ.* 44 (2022) 13, <https://doi.org/10.1186/s41021-022-00242-5>.
- J.C. Barrett, H. Vainio, D. Peakall, B.D. Goldstein, 12th meeting of the scientific group on methodologies for the safety evaluation of chemicals: susceptibility to environmental hazards, *Environ. Health Perspect.* 105 (1997) 699–737, <https://doi.org/10.1289/ehp.97105s4699>.
- J.M. Battershill, K. Burnett, S. Bull, Factors affecting the incidence of genotoxicity biomarkers in peripheral blood lymphocytes: impact on design of biomonitoring studies, *Mutagenesis* 23 (2008) 423–437, <https://doi.org/10.1093/mutage/gen040>.
- C. Ladeira, S. Viegas, Human Biomonitoring – an overview on biomarkers and their application in occupational and environmental health, *Biomonitoring* 3 (2016), <https://doi.org/10.1515/bimo-2016-0003>.
- M. Kirsch-Volders, M. Fenech, C. Bolognesi, Validity of the lymphocyte cytokinesis-block micronucleus assay (L-CBMN) as biomarker for human exposure to chemicals with different modes of action: a synthesis of systematic reviews, *Mutat. Res. Toxicol. Environ. Mutagen* 836 (2018) 47–52, <https://doi.org/10.1016/j.mrgentox.2018.05.010>.
- M. Fenech, Cytokinesis-block micronucleus cytome assay, *Nat. Protoc.* 2 (2007) 1084–1104, <https://doi.org/10.1038/nprot.2007.77>.
- M. Fenech, Cytokinesis-block micronucleus cytome assay evolution into a more comprehensive method to measure chromosomal instability, *Genes (Basel)* 11 (2020) 1203, <https://doi.org/10.3390/genes11101203>.
- C. Ladeira, L. Smajdova, The use of genotoxicity biomarkers in molecular epidemiology: applications in environmental, occupational and dietary studies, *AIMS Genet.* 04 (2017) 166–191, <https://doi.org/10.3934/genet.2017.3.166>.
- S. Sommer, I. Buraczewska, M. Kruszewski, Micronucleus assay: the state of art, and future directions, *Int. J. Mol. Sci.* 21 (2020) 1534, <https://doi.org/10.3390/ijms21041534>.
- Organization for Economic Co-operation and Development (OECD), Test No. 474: Mammalian Erythrocyte Micronucleus Test, OECD, 2016. <https://doi.org/10.1787/9789264264762-en>.
- M.J. Baker, J. Trevisan, P. Bassan, R. Bhargava, H.J. Butler, K.M. Dorling, P. R. Fielden, S.W. Fogarty, N.J. Fullwood, K.A. Heys, C. Hughes, P. Lasch, P. L. Martin-Hirsch, B. Obinaju, G.D. Sockalingum, J. Sulé-Suso, R.J. Strong, M. J. Walsh, B.R. Wood, P. Gardner, F.L. Martin, Using Fourier transform IR spectroscopy to analyze biological materials, *Nat. Protoc.* 9 (2014) 1771–1791, <https://doi.org/10.1038/nprot.2014.110>.
- G.J. Vazquez-Zapien, M.M. Mata-Miranda, V. Sanchez-Monroy, R.J. Delgado-Macuil, D.G. Perez-Ishiwara, M. Rojas-Lopez, FTIR spectroscopic and molecular analysis during differentiation of pluripotent stem cells to pancreatic cells, *Stem Cells Int* 2016 (2016) 1–10, <https://doi.org/10.1155/2016/6709714>.
- B. Ribeiro da Cunha, L.P. Fonseca, C.R.C. Calado, Simultaneous elucidation of antibiotic mechanism of action and potency with high-throughput Fourier-transform infrared (FTIR) spectroscopy and machine learning, *Appl. Microbiol. Biotechnol.* 105 (2021) 1269–1286, <https://doi.org/10.1007/s00253-021-11102-7>.
- Á. Novais, A.R. Freitas, C. Rodrigues, L. Peixe, Fourier transform infrared spectroscopy: unlocking fundamentals and prospects for bacterial strain typing, *Eur. J. Clin. Microbiol. Infect. Dis.* 38 (2019) 427–448, <https://doi.org/10.1007/s10096-018-3431-3>.
- C. Petitbois, G. Délérís, Analysis and monitoring of oxidative stress in exercise and training by FTIR spectrometry, *Int. J. Sports Physiol. Perform.* 3 (2008) 119–130, <https://doi.org/10.1123/ijssp.3.2.119>.
- S. Caliskan, H. Oldenhof, R. Brogna, B. Rashidfarokhi, H. Sieme, W.F. Wolkers, Spectroscopic assessment of oxidative damage in biomolecules and tissues, *Spectrochim. Acta Part A Mol. Biomol. Spectrosc.* 246 (2021), 119003, <https://doi.org/10.1016/j.saa.2020.119003>.
- D. Liu, S. Caliskan, B. Rashidfarokhi, H. Oldenhof, K. Jung, H. Sieme, A. Hilfinger, W.F. Wolkers, Fourier transform infrared spectroscopy coupled with machine learning classification for identification of oxidative damage in freeze-dried heart valves, *Sci. Rep.* 11 (2021) 12299, <https://doi.org/10.1038/s41598-021-91802-2>.
- E. Farhadi, F. Kobarfard, F.H. Shirazi, FTIR biospectroscopy investigation on cisplatin cytotoxicity in three pairs of sensitive and resistant cell line, *Iran. J. Pharm. Res.* 15 (2016) 213–220.
- P.L. Fale, A. Altharawi, K.L.A. Chan, In situ Fourier transform infrared analysis of live cells' response to doxorubicin, *Biochim. Biophys. Acta - Mol. Cell Res* 1853 (2015) 2640–2648, <https://doi.org/10.1016/j.bbamcr.2015.07.018>.
- C.L.M. Morais, R.F. Shore, M.G. Pereira, F.L. Martin, Assessing binary mixture effects from genotoxic and endocrine disrupting environmental contaminants using infrared spectroscopy, *ACS Omega* 3 (2018) 13399–13412, <https://doi.org/10.1021/acsomega.8b01916>.
- R. Araújo, L. Ramalheite, H. Paz, C. Ladeira, C.R.C. Calado, A new method to predict genotoxic effects based on serum molecular profile, *Spectrochim. Acta Part A Mol. Biomol. Spectrosc.* 255 (2021), 119680, <https://doi.org/10.1016/j.saa.2021.119680>.
- S.H. Rutherford, A. Nordon, N.T. Hunt, M.J. Baker, Biofluid analysis and classification using IR and 2D-IR spectroscopy, *Chemom. Intell. Lab. Syst.* 217 (2021), 104408, <https://doi.org/10.1016/j.chemolab.2021.104408>.
- A. Sala, D.J. Anderson, P.M. Brennan, H.J. Butler, J.M. Cameron, M.D. Jenkinson, C. Rinaldi, A.G. Theakstone, M.J. Baker, Biofluid diagnostics by FTIR spectroscopy: A platform technology for cancer detection, *Cancer Lett.* 477 (2020) 122–130, <https://doi.org/10.1016/j.canlet.2020.02.020>.
- H. Hamdi, Y. Ben Othmène, O. Ammar, A. Klifi, E. Hallara, F. Ben Ghali, Z. Houas, M.F. Najjar, S. Abid-Essefi, Oxidative stress, genotoxicity, biochemical and histopathological modifications induced by epoxiconazole in liver and kidney of Wistar rats, *Environ. Sci. Pollut. Res.* 26 (2019) 17535–17547, <https://doi.org/10.1007/s11356-019-05022-3>.
- D.C. Damasceno, Y.K. Sinzato, A. Bueno, B. Dallaqua, P.H. Lima, I.M.P. Calderon, M.V.C. Rudge, K.E. Campos, Metabolic profile and genotoxicity in obese rats exposed to cigarette smoke, *Obesity* 21 (2013) 1596–1601, <https://doi.org/10.1002/oby.20152>.
- S. García-Medina, M. Galar-Martínez, L.M. Gómez-Oliván, K. Ruiz-Lara, H. Islas-Flores, E. Gasca-Pérez, Relationship between genotoxicity and oxidative stress induced by mercury on common carp (*Cyprinus carpio*) tissues, *Aquat. Toxicol.* 192 (2017) 207–215, <https://doi.org/10.1016/j.aquatox.2017.09.019>.
- M.O. Ansari, N. Parveen, M.F. Ahmad, A.L. Wani, S. Afrin, Y. Rahman, S. Jameel, Y. A. Khan, H.R. Siddique, M. Tabish, G.G.H.A. Shadab, Evaluation of DNA interaction, genotoxicity and oxidative stress induced by iron oxide nanoparticles both in vitro and in vivo: attenuation by thymoquinone, *Sci. Rep.* 9 (2019) 6912, <https://doi.org/10.1038/s41598-019-43188-5>.
- B. Aydın, Z. Atlı Şekeröglü, V. Şekeröglü, Acrolein-induced oxidative stress and genotoxicity in rats: protective effects of whey protein and conjugated linoleic acid,



- Drug Chem. Toxicol. 41 (2018) 225–231, <https://doi.org/10.1080/01480545.2017.1354872>.
- [30] S. Shadnia, E. Azizi, R. Hosseini, S. Khoei, S. Fouladdel, A. Pajoumand, N. Jalali, M. Abdollahi, Evaluation of oxidative stress and genotoxicity in organophosphorus insecticide formulators, *Hum. Exp. Toxicol.* 24 (2005) 439–445, <https://doi.org/10.1191/0960327105ht5490a>.
- [31] M. Cengiz, V. Sahinturk, S.C. Yildiz, I.K. Şahin, N. Bilici, S.O. Yaman, Y. Altuner, S. Appak-Baskoy, A. Ayhanci, Cyclophosphamide induced oxidative stress, lipid per oxidation, apoptosis and histopathological changes in rats: protective role of boron, *J. Trace Elem. Med. Biol.* 62 (2020), 126574, <https://doi.org/10.1016/j.jtemb.2020.126574>.
- [32] A.J. Akamo, D.I. Akinloye, R.N. Ugbaja, O.O. Adeleye, O.A. Dosumu, O.E. Eteng, M.C. Antiya, G. Amah, O.A. Ajayi, S.O. Faseun, Naringin prevents cyclophosphamide-induced erythrocytotoxicity in rats by abrogating oxidative stress, *Toxicol. Rep.* 8 (2021) 1803–1813, <https://doi.org/10.1016/j.toxrep.2021.10.011>.
- [33] D. Zeng, Y. Wang, Y. Chen, D. Li, G. Li, H. Xiao, J. Hou, Z. Wang, L. Hu, L. Wang, J. Li, Angelica Polysaccharide Antagonizes 5-FU-Induced Oxidative Stress Injury to Reduce Apoptosis in the Liver Through Nrf2 Pathway, *Front. Oncol.* 11 (2021), <https://doi.org/10.3389/fonc.2021.720620>.
- [34] S. Numazawa, K. Sugihara, S. Miyake, H. Tomiyama, A. Hida, M. Hatsuno, M. Yamamoto, T. Yoshida, Possible Involvement of oxidative stress in 5-fluorouracil-mediated myelosuppression in Mice, *Basic Clin. Pharmacol. Toxicol.* 108 (2011) 40–45, <https://doi.org/10.1111/j.1742-7843.2010.00621.x>.
- [35] Y.Ç. Kumbul, M. Naziroğlu, Paclitaxel promotes oxidative stress-mediated human laryngeal squamous tumor cell death through the stimulation of calcium and zinc signaling pathways: no synergic action of melatonin, *Biol. Trace Elem. Res.* 200 (2022) 2084–2098, <https://doi.org/10.1007/s12011-022-03125-6>.
- [36] N.A. Duggett, L.A. Griffiths, O.E. McKenna, V. de Santis, N. Yongsanguanchai, E. B. Mokori, S.J.L. Flatters, Oxidative stress in the development, maintenance and resolution of paclitaxel-induced painful neuropathy, *Neuroscience* 333 (2016) 13–26, <https://doi.org/10.1016/j.neuroscience.2016.06.050>.
- [37] C. Ladeira, S. Viegas, M. Pádua, M. Gomes, E. Carolino, M.C. Gomes, M. Brito, Assessment of genotoxic effects in nurses handling cytostatic drugs, *J. Toxicol. Environ. Heal. Part A* 77 (2014) 879–887, <https://doi.org/10.1080/15287394.2014.910158>.
- [38] C. Ladeira, S. Viegas, M. Pádua, E. Carolino, M.C. Gomes, M. Brito, Relation between DNA damage measured by comet assay and OGG1 Ser326Cys polymorphism in antineoplastic drugs biomonitoring, *AIMS Genet* 02 (2015) 204–218, <https://doi.org/10.3934/genet.2015.3.204>.
- [39] J.A., J. Trygg, J. Gullberg, A.I. Johansson, P. Jonsson, H. Antti, S.L. Marklund, T. Moritz, Extraction and GC/MS analysis of the Human Blood Plasma Metabolome, *Anal. Chem.* 77 (2005) 8086–8094, <https://doi.org/10.1021/ac051211v>.
- [40] M. Fenech, N. Holland, W.P. Chang, E. Zeiger, S. Bonassi, The human micronucleus project—an international collaborative study on the use of the micronucleus technique for measuring DNA damage in humans, *Mutat. Res. Mol. Mech. Mutagen* 428 (1999) 271–283, [https://doi.org/10.1016/S1383-5742\(99\)00053-8](https://doi.org/10.1016/S1383-5742(99)00053-8).
- [41] S. Viegas, M. Pádua, A.C. Veiga, E. Carolino, M. Gomes, Antineoplastic drugs contamination of workplace surfaces in two Portuguese hospitals, *Environ. Monit. Assess.* 186 (2014) 7807–7818, <https://doi.org/10.1007/s10661-014-3969-1>.
- [42] T. Gulten, E. Evke, I. Ercan, T. Evrensel, E. Kurt, O. Manavoglu, Lack of genotoxicity in medical oncology nurses handling antineoplastic drugs: Effect of work environment and protective equipment, *Work* 39 (2011) 485–489, <https://doi.org/10.3233/WOR-2011-1198>.
- [43] P.J.M. Sessink, R.P. Bos, Drugs hazardous to healthcare workers, *Drug Saf.* 20 (1999) 347–359, <https://doi.org/10.2165/00002018-199920040-00004>.
- [44] Occupational dermal exposure to cyclophosphamide in dutch hospitals: a pilot study, *Ann. Occup. Hyg.* (2004), <https://doi.org/10.1093/annhyg/meh017>.
- [45] B. Laffon, J.P. Teixeira, S. Silva, J. Loureiro, J. Torres, E. Pásaro, J. Méndez, O. Mayan, Genotoxic effects in a population of nurses handling antineoplastic drugs, and relationship with genetic polymorphisms in DNA repair enzymes, *Am. J. Ind. Med.* 48 (2005) 128–136, <https://doi.org/10.1002/ajim.20189>.
- [46] N. Kopjar, V. Garaj-Vrhovac, V. Kašuba, R. Rozgaj, S. Ramić, V. Pavlica, D. Želježić, Assessment of genotoxic risks in Croatian health care workers occupationally exposed to cytotoxic drugs: a multi-biomarker approach, *Int. J. Hyg. Environ. Health* 212 (2009) 414–431, <https://doi.org/10.1016/j.ijheh.2008.10.001>.
- [47] A.F. Aristizabal-Pachon, W.O. Castillo, Genotoxic evaluation of occupational exposure to antineoplastic drugs, *Toxicol. Res.* 36 (2020) 29–36, <https://doi.org/10.1007/s43188-019-00003-7>.
- [48] A. Fucic, A. Jazbec, A. Mijic, D. Šešo-Šimic, R. Tomek, Cytogenetic consequences after occupational exposure to antineoplastic drugs, *Mutat. Res. Toxicol. Environ. Mutagen* 416 (1998) 59–66, [https://doi.org/10.1016/S1383-5718\(98\)00084-9](https://doi.org/10.1016/S1383-5718(98)00084-9).
- [49] H. Deng, M. Zhang, J. He, W. Wu, L. Jin, W. Zheng, J. Lou, B. Wang, Investigating genetic damage in workers occupationally exposed to methotrexate using three genetic end-points, *Mutagenesis* 20 (2005) 351–357, <https://doi.org/10.1093/mutage/gei048>.
- [50] D. Cavallo, C.L. Ursini, E. Omodeo-Salè, S. Iavicoli, Micronucleus induction and FISH analysis in buccal cells and lymphocytes of nurses administering antineoplastic drugs, *Mutat. Res. Toxicol. Environ. Mutagen* 628 (2007) 11–18, <https://doi.org/10.1016/j.mrgentox.2006.10.014>.
- [51] S. Bouraoui, A. Brahem, F. Tabka, N. Mrizek, A. Saad, H. Elghezal, Assessment of chromosomal aberrations, micronuclei and proliferation rate index in peripheral lymphocytes from Tunisian nurses handling cytotoxic drugs, *Environ. Toxicol. Pharmacol.* 31 (2011) 250–257, <https://doi.org/10.1016/j.etap.2010.11.004>.
- [52] A.A. El-Ebiary, A.A. Abuelfadl, N.I. Sarhan, Evaluation of genotoxicity induced by exposure to antineoplastic drugs in lymphocytes of oncology nurses and pharmacists, *J. Appl. Toxicol.* 33 (2013) 196–201, <https://doi.org/10.1002/jat.1735>.
- [53] D.K.R. Medipally, T.N.Q. Nguyen, J. Bryant, V. Untereiner, G.D. Sockalingum, D. Cullen, E. Noone, S. Bradshaw, M. Finn, M. Dunne, A.M. Shannon, J. Armstrong, F.M. Lyng, A.D. Meade, Monitoring radiotherapeutic response in prostate cancer patients using high throughput FTIR spectroscopy of liquid biopsies, *Cancers (Basel)* 11 (2019) 925, <https://doi.org/10.3390/cancers11070925>.
- [54] J. Titus, H. Ghimire, E. Viennois, D. Merlin, A.G. Unil Perera, Protein secondary structure analysis of dried blood serum using infrared spectroscopy to identify markers for colitis screening, *J. Biophotonics* 11 (2018), <https://doi.org/10.1002/jbio.201700057>.
- [55] H. Ghimire, M. Venkataramani, Z. Bian, Y. Liu, A.G.U. Perera, ATR-FTIR spectral discrimination between normal and tumorous mouse models of lymphoma and melanoma from serum samples, *Sci. Rep.* 7 (2017) 16993, <https://doi.org/10.1038/s41598-017-17027-4>.
- [56] G. Bellisola, C. Sorio, *Infrared spectroscopy and microscopy in cancer research and diagnosis*, *Am. J. Cancer Res.* 2 (2012) 1–21.
- [57] B. Udvardi, I.J. Kovács, T. Fancsik, P. Kónya, M. Bátorfi, F. Stercel, G. Falus, Z. Szalai, Effects of particle size on the attenuated total reflection spectrum of minerals, *Appl. Spectrosc.* 71 (2017) 1157–1168, <https://doi.org/10.1177/0003702816670914>.
- [58] A. Kohler, U. Böcker, J. Warringer, A. Blomberg, S.W. Omholt, E. Stark, H. Martens, Reducing Inter-Replicate Variation in Fourier Transform Infrared Spectroscopy by Extended Multiplicative Signal Correction, *Appl. Spectrosc.* 63 (2009) 296–305, <https://doi.org/10.1366/000370209787598906>.